Effects of size and site factors on the availability of a standalone microgrid

A.Abdulkarim, S. M. Abdelkader[2] , D. J. Morrow[3]
[1]Department of Electrical & Electronics Engineering, University of Ilorin, Nigeria
[2]Electrical Engineering Department, Mansoura University, Mansoura 35516 Egypt
[3]School of Electronics, Electrical Engineering and Comp Sci. QUB, United Kingdom
abkzarewa@yahoo.com[1]; s.abdelkader@qub.ac.uk[2]; dj.morrow@ee.qub.ac.uk[3]

\

Abstract

In this paper, effects of storage and diesel generator on the availability hybrid renewable energy microgrid have been investigated. Markov technique has been used for the analysis of the output powers of the wind energy conversion system (WECS) and solar energy conversion system (SECS).The proposed method has been tested by increasing the rated power of the WECS and SECS by 25 %, 50%, 75% and 100%. The results have shown a decreased in the number of times a diesel generator starts by 2 %, 7%, 9% and 9 % for WECS. Similarly, SECS decreased same by 4 %, 8 %, 11%, and 13 %. Also, the study of wind generator parameter at different cut-in-speeds levels, including 2 m/s, 2.5m/s, 3.5m/s and 4 m/s reduced the number of times a diesel generator start by 122, 147, 116 and 134. In addition, the effects of weather on the availability of system have been investigated using Boolean Logic Driven Markov process. In the same way, neglecting weather factor overestimate the system availability by 3.55%. Also, increasing the rated power of the WECS is the best way of maximizing the benefit-to-cost ratio (BCR) of the system.
Keywords---Microgrid, renewable energy, wind storage diesel generator, availability weather, PV

Introduction

Recently, integrating an existing diesel generator with renewable energy such as wind and solar in the form of a microgrid is being planned for isolated loads. In some cases, battery storage is added to reduce the variations in power from the renewable energy. In this arrangement, the diesel generator operates only when all the other resources cannot meet the demand. The operation of the battery storage and diesel generator may have effects on the economy and availability of the system. This makes the development of strategies for maximising the benefits of these units an important priority for system planners.

This paper investigated the factors that will maximise the benefits of storage and diesel generators connected to an isolated microgrid. The study is divided into two sections. Section one study the effects of the renewable energy resource on the operation of a diesel generator. The relationship between the availability of the storage and the availability of the microgrid have been analysed in section two. In order to achieve these, Markov and Boolean logic driven Markov processes are used in order to take the randomness of the renewable energy power output into consideration. This is achieved by representing the output power of the WECS (wind energy conversion system) and SECS (solar energy conversion system) using a transition matrix. The elements of this matrix are the transition rates between the different power output levels of the WECS and SECS. Such presentations enable incorporating the failure rate of both solar and wind energy conversion systems in the power classes. The output of the classification is used to develop a Markov model whose solution is used to estimate the system parameters. ***The parameters include the number of times a diesel generator starts, the energy produced and the energy used by the system. Additionally, the effects of site and size factors on the number of times a diesel generator starts are investigated.*** Finally, since the system may be exposed to bad weather, the effects of weather on the availability need to be known in order to deliver autonomous, economical and reliable energy to the isolated systems.

1. Analyses of the renewable energy resources

The hourly renewable energy power of the study area is obtained by adding the hourly output power of the WECS and SECS. It is assumed that modelling this way takes the hourly fluctuations of both the wind and solar energy conversion systems into consideration. WECS system output power is a function of the three wind speeds that results in

different design alternatives(Yang, Pei, & Qi, 2012). The wind speeds include cut-in speed (V_{ci}), cut-out speed(V_{co}) and the rated speed of

$$P(v) = \begin{cases} P_r \cdot \dfrac{V_l - V_{cl}}{V_r - V_{ci}} & V_{cl} < V < V_r \\ P_r & V_r \le V < V_{co} \\ 0 & V \le V_{ci} \text{ or } V \ge V_{co} \end{cases}$$

The wind turbine considered is assumed to be highly reliable and compact in size. It is considered ideal for both populated and remote areas due to the compact size that make it easy to transport. It has a rated power of 850 kW(Manco & Testa, 2007). The proposed wind turbine has the ability to

the wind turbine (V). The power output of the wind energy conversion system is obtained using

(1)

optimise the output power using pitch technology in both high and medium wind speed conditions. It is also available in various tower heights and the characteristics of this wind turbine are shown in Table   1.

Table 1: Wind turbine specification.

Cut-in-speed (m/s)	Normal wind speed (m/s)	Cut-out- speed (m/s)
4	16	25

On the other hand, the output power of the SECS can be determined from different mathematical models expressed in (Yang, Pei, & Qi, 2012)-(Zhao, Xuesong, Jian, Caisheng, & Li, 2013). In these models, the output power of the system can be determined depending on some parameters. These parameters include its rated power under standard test condition, light intensity, and the operating ambient temperature. The model used in the determination of the output power of the solar energy conversion system is expressed in equation (2).

$$P_{PV} = \eta_g A_m N_{PV} G_t \qquad (2)$$

where, G_t is the solar radiation of the operating point ($[w/m]^2$) , η_g is the instantaneous PV generator efficiency, A_m is the area of a single

module used in the analysis (m^2) and N_{PV} is the number of module. The module efficiency can be determined based on the mathematical model defined in (Tafreshi, Zamani, Ezzati, & Vahedi, 2010)

Renewable energy potential of Belfast, United Kingdom is used in the analysis. Application of the wind turbine characteristic and site wind speed result in the output power of the WECS. Similar analysis is carried out for the SECS. Finally, the total hourly output power of the renewable energy side of the proposed system is shown in Figure 1.The hourly output power of the renewable energy systems is obtained by summing the output power of the wind and solar energy systems, as shown in Figure   1.
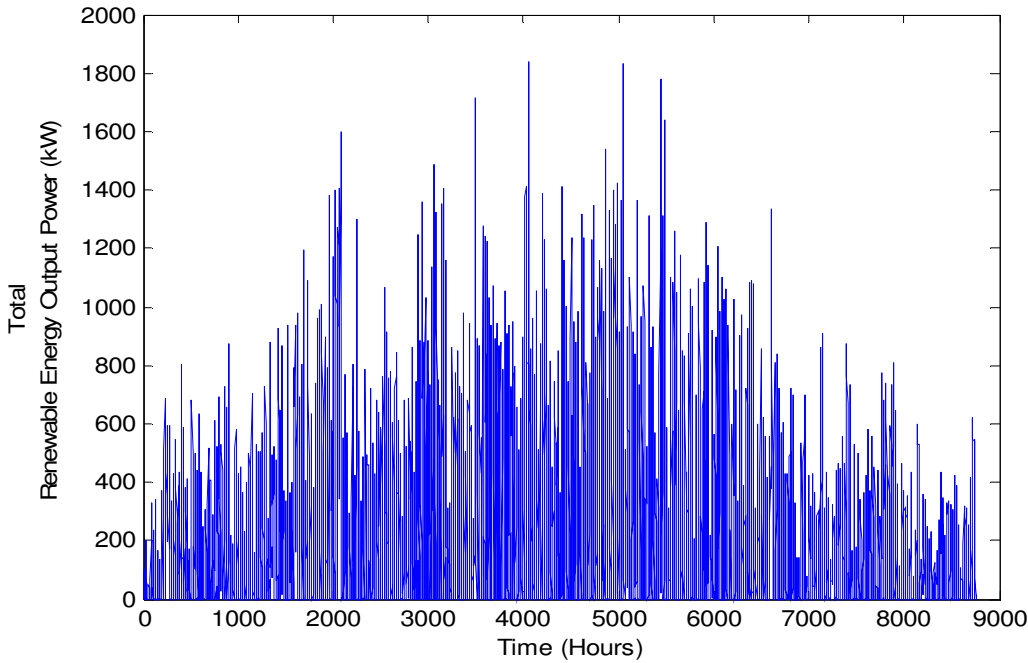
Figure 1: Total renewable energy output power.

2. Modelling of the renewable energy output power

The output power of the renewable energy system is used to derive the renewable energy power classes P_0-P_{10}. In addition, the output power is used to assume a class interval of 200 kW span between P_1 and P_9. On the other hand, P_0 represent a class with output power equal to zero and P_{10} is the class of outputs greater 1600 kW and less than or equal to the 1836 kW. These are used to define the powers in each class according as shown in Table 2. In each class the minimum power is defined as (Pmin), the upper limit is called the maximum power (Pmax) and the mean power in each class is defined as (Pmean) of the class. In order to treat the output power statistically, the transition rates among different states (different power classes) are determined

from the power output of the system. The expressions for the determination of the transition rates are given by Equations (3) and (4).

$$\varphi_{ij\neq j} = \frac{n_{ij}/N_T}{N_i/N_T} \cdot \frac{1}{\Delta t} \quad \text{[events/hour]} \quad (3)$$

$$\varphi_{ij} = 1 - \sum \varphi_{ij\neq j} \quad (4)$$

where φ_{ij} is the transition rate between state i and the state j

Δt is the is considered as one hour,

The result of Equations (3) and (4) is presented in Table 3, the row represents the i state and the column of the j state.

Table 2: Total renewable energy output power classifications.

Power Class	Pmin	Pmax	Pmean	Sample in the Class	Class frequency
P_0	0	0	0	1327	0.1515
P_1	0	200	200	738	0.0842
P_2	200	400	300	142	0.0162
P_3	400	600	500	789	0.0901
P_4	600	800	700	999	0.1140
P_5	800	1000	900	791	0.0903
P_6	1000	1200	1100	458	0.0523

P_7	1200	1400	1300	764	0.0872
P_8	1400	1600	1500	1375	0.1570
P_9	1600	1836	1718	607	0.0693
P_{10}	1836	1836	1836	770	0.0879

Table 3: Transition rates between power classes.

	0	1	2	3	4	5	6	7	8	9	10
0	0.3926	0.2724	0	0.2269	0.2342	0.2149	0.2205	0.25	0.3513	0.3328	0.4792
1	0.3406	0.2696	0.6197	0.3194	0.2533	0.2807	0.2795	0.3442	0.312	0.3328	0.3662
2	0.1771	0.1816	0.1761	0.2231	0.1832	0.177	0.1354	0.1649	0.176	0.201	0.1247
3	0.0799	0.1328	0.1268	0.1242	0.1532	0.1252	0.1376	0.0864	0.0865	0.0923	0.0273
4	0.0083	0.061	0.0211	0.076	0.0991	0.1024	0.1026	0.0654	0.0313	0.0379	0.0026
5	0.0015	0.0474	0.0141	0.0228	0.0501	0.0594	0.059	0.0445	0.0291	0.0033	0
6	0	0.0217	0.007	0.0038	0.013	0.019	0.0459	0.0275	0.0116	0	0
7	0	0.0108	0.007	0.0038	0.009	0.0152	0.0131	0.0092	0.0022	0	0
8	0	0.0027	0.0282	0	0.003	0.0038	0.0044	0.0039	0	0	0
9	0	0	0	0	0.002	0.0013	0	0.0039	0	0	0
10	0	0	0	0	0	0.0013	0.0022	0	0	0	0

3. Markovian model

In order to analyse the hybrid microgrid using a Markov process, the model presented in Figure 2 is proposed. The model consists of the output power of the two renewable energy resources. Each state corresponds to a class with the corresponding output power levels of the state. Modelling this way makes it possible to observe the transition between states.
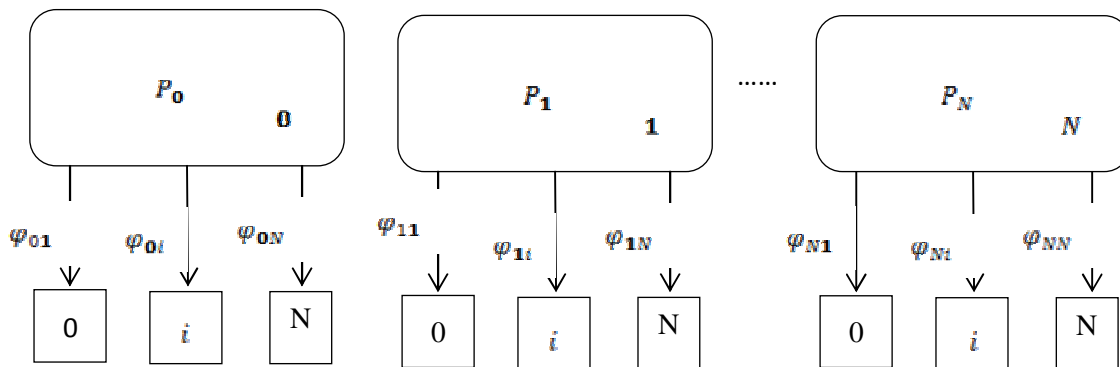

Figure 2: Markov model of hybrid PV-wind Microgrid.

4. Solution of the proposed model

The solution of the proposed model is based on the expressions of the steady state probabilities, durations and frequencies of entry into the states. The mathematical expressions of these variables are described in (Manco & Testa, 2007). Also, the state probabilities are defined using the relationships between the input and output frequencies of each state.

$$\alpha_1 \cdot \sum_{\substack{j=1 \\ j \neq 1}}^{N} \varphi_{1j} = \sum_{\substack{j=1 \\ j \neq 1}}^{N} \alpha_j \cdot \varphi_{j1}$$

$$\alpha_2 \cdot \sum_{\substack{j=1 \\ j \neq 2}}^{N} \varphi_{1j} = \sum_{\substack{j=1 \\ j \neq 2}}^{N} \alpha_j \cdot \varphi_{j2}$$

$$\cdots\cdots\cdots\cdots\cdots\cdots\cdots\cdots\cdots\cdots\cdots$$

$$\alpha_N \cdot \sum_{\substack{j=1 \\ j \neq N}}^{N} \varphi_{1j} = \sum_{\substack{j=1 \\ j \neq N}}^{N} \alpha_j \cdot \varphi_{jN}$$

(5)

It can be observed that these are systems of linear Equations of N unknowns. In this case, the unknowns are $\alpha_1, \alpha_2 - - - \alpha_N$. Eliminating the last equation and adding it to the steady state probability, the steady state probabilities are given by Equation (6).

$$\sum_{i=1}^{N} \alpha_i = 1$$

(6)

The system frequency is determined using Equation (7).

$$f_i = \alpha_i \cdot \sum_{\substack{j=1 \\ j \neq 2}}^{N} \varphi_{ij} \quad i = 1, 2 \dots N$$

(7)

Finally the mean state durations $d_1, \quad d_2 \dots d_N$ are determined directly from the transition rate using the expressions described in Equation (8).

$$d_i = 1 \Bigg/ \sum_{\substack{j=1 \\ j \neq i}}^{N} \varphi_{ij} \quad i = 1, 2 \dots N$$

(8)

In order to test the application of the procedure, the proposed model has been implemented. The result is shown in Table 4.

Table 4: Steady state solution of the model.

Power Class	Pmin	Pmax	Pmean	Steady State Probability	Duration (Hours) m_r.	Frequency (Event/hour) f_r.
P0	0	0	0	0.1615	1.6464	0.0920
P1	0	200	200	0.0842	1.3692	0.0615
P2	200	400	300	0.0162	1.2137	0.0134
P3	400	600	500	0.0901	1.1418	0.0789
P4	600	800	700	0.1140	1.1100	0.1027
P5	800	1000	900	0.0903	1.0632	0.0849
P6	1000	1200	1100	0.0523	1.0481	0.0499
P7	1200	1400	1300	0.0872	1.0092	0.0864
P8	1400	1600	1500	0.1570	1.0000	0.1570
P9	1600	1836	1718	0.0693	1.0000	0.0693
P10	1836	1836	1836	0.0879	1.0000	0.0879

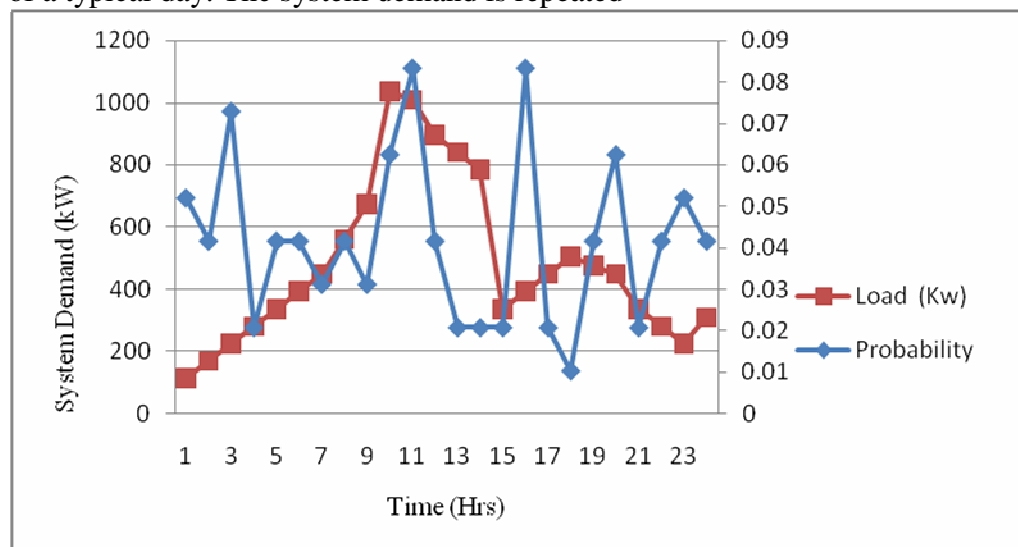Figure 3 shows the load profile and the probability of occurrences for each load demand for a period of a typical day. The system demand is repeated for a period of one year and is used in the simulation.

Figure 3: Daily demand and probability at each hour.

For the load distribution, the daily energy need of the system is obtained using equation (9).

$$E_{Lj} = P_{Lj} \cdot T_{Lj} \ [kWh]$$ (9)

The annual energy need by the system is determined using Equation (10).

$$E_{Lj} = 365 \cdot \sum_{j=1}^{N} P_{Lj} \cdot T_{Lj}$$ (10)

Comparing the output power of the renewable energy sources shown in Figure 1 and the system demand in Figure 3; it can be observed that there is a need for storage and a diesel generator

If the $\Delta P > 0$ and the battery is not fully charged, the battery absorbs the difference in power.

On the other hand, when $\Delta P < 0$, the following strategy applied that is depending on the dispatch strategy:

If the battery is able to supply the deficit, the diesel generator turns off.

$$P_b(i) = \Delta P(i)$$

Application of the algorithm presented results into new output power. The new system output power for the renewable energy and the battery storage is shown in Figure 4. The output of the simulation shows that the output power generated by the renewable energy sources is stored for use at another time. In addition, the result has shown the need for the diesel generator.

Algorithm for adding the storage and diesel generator

In order to integrate both storage and diesel generator, the following algorithm is implemented. Since the amount of energy stored is time dependant, the input/output power of the battery is controlled by the following algorithm,

$$\Delta P = PRE - Pl$$

where

$$Pl = \frac{Pload}{\eta_{inv}}$$

where $Pload$ is the power demanded by the load, and η_{inv} is efficiency of the DC/AC inverter, which is usually specified by the manufacturer. Depending on the manufacturer's recommendation and on the ΔP value, the following strategy is applied:
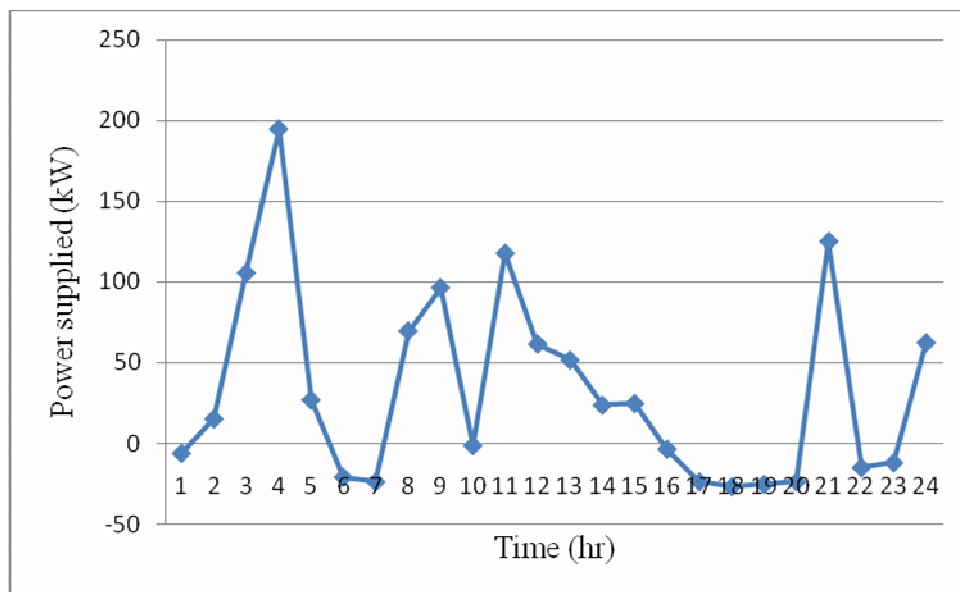

Figure 4: New power profile without diesel generator.

If the battery cannot supply the demand, it is assumed that the battery is neither charging nor discharging, and therefore the diesel generator is turned ON and is supplying the deficit.

$$P_{DG}(i) = \Delta P(i)$$

The proposed algorithm is used to estimate the number of times a diesel generator starts. Different

alternatives for reducing the number of times a diesel generator starts could be proposed. This will maximize the lifespan of the diesel generator, and the economic benefit of the system might be improved. The alternative includes the effects of the size and site factors on the annual number of times the diesel generator starts.

5.   Effects of size factors on the diesel generator operation

This section investigates the relationship between the size factors and the operation of the diesel generator. The analysis is proposed in order to recommend ways of maximising the benefits of size factors on the diesel generator operation. The effects come down to the rated power of the WECS and SECS. Various case studies considered include the base case in which the actual renewable energy sizes of the WECS and SECS are used. The base case is followed by cases II, III, IV and V for 25%, 50%, 75% and 100% increases in size factors.

The results of the simulations are presented as a percentage of the base case, as shown in Figure 5. The results have shown that increasing the rated power of the WECS and SECS by 25% decreased the number of times a diesel generator starts by 2% and 4% respectively. Similarly, increasing the rated power in the same order by 50% results in 7% and 8% decreases in the number of times the diesel generator starts. In the same way, increasing the rated power by 75% decreased the number by 9% and 11% respectively. Also, increasing the rated power of the WECS and SECS by 100% decreased the number of times the diesel generator starts by only 9% and 13% respectively. Increasing the rated power of SECS has the highest percentage decrease in the number of times the diesel generator starts. However, the benefit of the system is not proportional to the corresponding increase in the rated power of the WECS and SECS. Increases in the rated power of the WECS and SECS do not produce corresponding decreases in the number of times a diesel generator starts by the same factor.
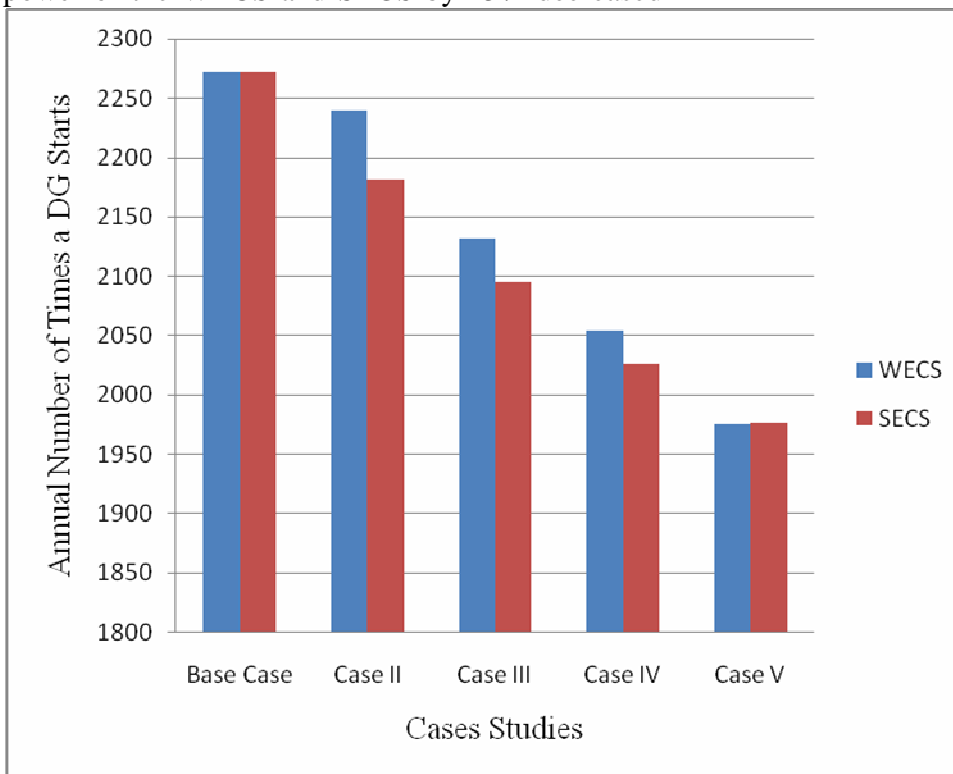

Figure 5: Number of diesel generator starts VS rated power of WECS & SECS.

6.   Effects of the site factor on diesel generator operation

Another factor used in the analysis of the proposed hybrid microgrid is the cut-in speed of the wind turbine generator. The cut-in-speed affects the number of times the diesel generator starts. This section explored how variations of the cut-in speed affect the number times a diesel generator starts. To achieve this aim, the cut-in
.

speed of the wind turbine is varied according to the proposed strategies. The proposed strategy in this case is to change the cut-in speed at different levels, including 2.0, 2.5, 3.0, 3.5 and 4.0 m/s. The result of this analysis is shown in Figure 6. Hence it can be seen that the best system benefit is obtained when the cut-in speed is 4 m/s
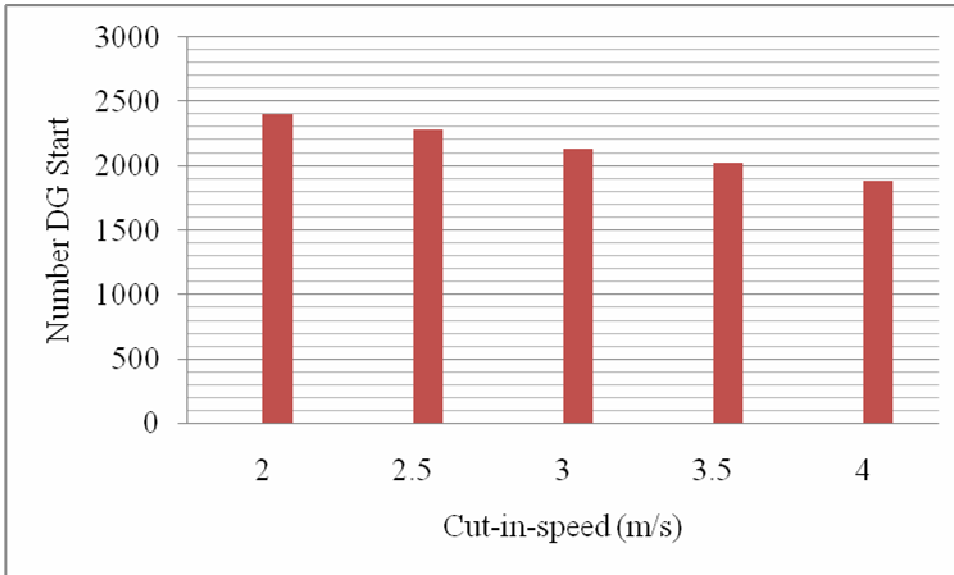
Figure 6: Effects of cut-in-speed on the DG start.

7. Benefits of storage on the net savings of hybrid microgrid

The output power of the renewable energy depends on the failure and repair rates of both the WECS and the SECS. Therefore a model that takes the failure and a repair rate into consideration is proposed in Figure 7(Abdelkader, 2013). This presentation enables us to use series and parallel theorems in the determination of the failure and repair rates of the system (Billinton & Allan, 1983). Modelling this way enables using a Markov theorem for the determination of the capacity of the storage system so that it would have economic value. In order to use the proposed method, the output power of the renewable energy sources is represented by the 3-state Markov model.
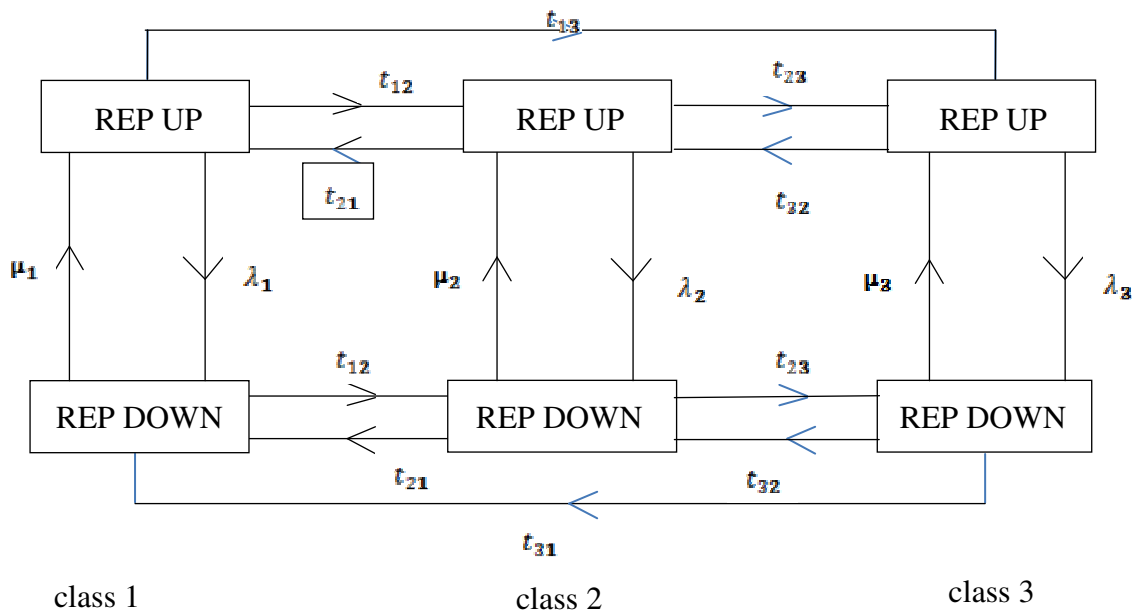
Figure 7: Proposed Markov model.
where, REP is the renewable energy output power

The proposed model can be represented mathematically in two different forms. The first presentation is to drive the system transition matrix and obtain the probability distributions of state at times k+1 in terms of the preceding state k. The second alternative is to drive the state equations by using the state diagram. The latter option has the advantage of reducing the order of equations by one half (Abdelkader, 2013). Therefore, the developed model is solved according to the second

method. The state equation of the Markov process consisting of three different renewable output powers is defined by:

$$
\begin{bmatrix} \dot{p_1} \\ \dot{p_2} \\ \dot{p_3} \\ \dot{q_1} \\ \dot{q_2} \\ \dot{q_1} \end{bmatrix} = \begin{bmatrix} -t_{12}-\lambda_1 -t_{13} & t_{21} & t_{31} & \mu_1 & 0 & 0 \\ t_{12} & -t_{12}-\lambda_1 -t_{13} & t_{32} & 0 & \mu_2 & 0 \\ t_{13} & t_{23} & -t_{12}-\lambda_1 -t_{13} & 0 & 0 & \mu_3 \\ \lambda_1 & 0 & 0 & -t_{12}-\lambda_1 -t_{13} & t_{21} & t_{31} \\ 0 & \lambda_2 & 0 & t_{12} & -t_{12}-\lambda_1 -t_{13} & t_{32} \\ 0 & 0 & \lambda_3 & t_{13} & t_{23} & -t_{12}-\lambda_1 -t_{13} \end{bmatrix} \begin{bmatrix} p_1 \\ p_2 \\ p_3 \\ q_1 \\ q_2 \\ q_3 \end{bmatrix}
$$

(11)

The probabilities of the output power of the renewable energy system are represented by P_1, P_2, P_3 for states 1, 2 and 3 respectively. The corresponding failure probabilities of the three states are represented by q_1, q_2, q_3. In the same way, the transition rate of each state is given as $t_{i,j}$, for states i to j respectively. According to the proposed model, it is can be seen that states 3, 4, 5 and 6 have equal power levels, all equal to zero. These states can be lumped together in order to reduce the number of equations. State 3 has zero output power due to low wind speed and low solar radiation. On the other hand, states 4, 5 and 6 have zero output power due to failures of the WECS and/or of the SECS. Mathematical expressions of the new states are given in Equation (12),

$$[\dot{P}] = [A][P]$$

(12)

where $[P] = [P_1 P_2 P_3 q_1 q_2 q_3]^T$

Equation (12) can be presented in a reduce form as:

$$[\dot{P}] = [B][P]$$

(13)

In this case, $[B] = [P_1 P_2 q]^T$, and q is the probability of the lumped states. The elements of the B matrix are determined as follows:

$b_{ij} = a_{ij} \ i = 1,2$ and $j = 1,2$

$$b_{3j} = \sum_{i=3}^{6} a_{ij} \ j = 1,2$$

$$b_{i3} = \frac{a_{i3} \cdot P_3(\infty) + \sum_{j=4}^{6} a_{ij} \cdot a_{j-3}(\infty)}{P_3(\infty) + \sum_{j=4}^{6} q_{j-3}(\infty)}$$

Also, (∞) is the steady states probability of p and q

$$b_{33} = -\sum_{i=1}^{2} b_{i3}$$

Presentation of the model in the reduced states enables us to determine the average time spent before the output power of the WECS and SECS drop from a specified value to zero. This time is used for the determination of the storage capacity required so that it has capacity credit. The aim is to determine the storage capacity that could be used for the maximum net savings.

8.1 Average return time

From the state equation

$$[\dot{P}] = [A][P]$$

(14)

taking the Laplace transform of both sides and assuming the initial state probabilities $[P(0)]$, the solution is given by

$$[P(t)] = L^{-1}[SI - B]^{-1}.[P(0)]$$

(15)

Hence Equation (15) expresses the probability of being in each state as a function of time. In order to solve this equation, it is assumed that the system starts from the down state. That means $P_1 = P_2 = 0$ and q or $P_3 = 1$. Having obtained the probabilities, the average output power at each interval is obtained from

$$P_o(t) = P_{av1}.P_1(t) + P_{av2}.P_2(t) + P_{av3}.P_3(t)$$

(16)

where $P_{av1}, P_{av2}, and \ P_{av3}$ are the average output power for classes 1, 2 and 3 respectively.

At any output power level, the average return time is obtained by solving Equation (17).

$$P_L = P_{av1} \cdot P_1(t) + P_{av2} \cdot P_2(t) + P_{av3} \cdot P_3(t)$$
(17)

Therefore, the storage capacity (Q) required to achieve capacity credit is determined by solving Equation (18).

$$Q = \int_0^{t_{av}} (P_L - P_{av3})dt$$
(18)

This section obtained the optimum storage capacity that needs to be added to the system so that it will have capacity credit. To achieve this, the analysis is divided into two sections. Section one determined the total annual system cost; this is the cost of the renewable energy resources and storage system. The second section obtained the total savings that maximised the capacity credit. In order to determine total savings, the total cost of the system is defined in Equation (19).

$$C = C_S * P_{rs} + C_W * P_{rw} + C_{ST} * Q_{ST}$$ (19)

Annual cost is estimated using the expression(Zhao, Zhang, Chen, Wang, & Guo, 2013)

$$P = A_n \cdot (1+e) \frac{\left|\frac{1+e}{1+i}\right|^y - 1}{1-e}$$
(20)

where A_n is the annual cost, P is the present value, i is the interest rate, y is the useful life years and e is the inflation rate.

8.2 Savings

The savings as a result of the proposed storage is divided into two parts consisting of the avoided cost of displaced capacity and the cost of energy saved. The avoided cost of the displaced conventional capacity is defined in Equation (21)

$$CC = CC_o * CP_d$$
(21)

where

CC : annual savings due to the displaced capacity

CC_o: the annual cost of kW of the displaced capacity

CP_d: the displaced capacity kW

To determine the cost of energy saved, the following assumptions are applied. If the renewable energy systems have no storage system, then the output energy cannot be scheduled. Therefore the savings are determined based on the peak load. Alternatively, if storage is added, then the firm capacity is only a fraction of the rated power. The energy output is evaluated as a fraction of the peak energy price, and the energy saved is defined as

$$ES = (CP_d * CF_1 + (P_{av} - CP_d) * CF_2) * 8760$$
(22)

The total savings are:

$$TS = CC + ES$$
(23)

8.3 Application of the procedure

The application of the proposed procedure is tested using renewable output power of the model and the cost data shown in Table 5.

Table 5: Cost data for the benefits of storage system.

Interest rate	0.40%
Inflation rate	0.50%
On peak energy price	0.2724 $/kWh
Off peak energy prices	0.1369 $/kWh
Cost of WECS	4700 $/kW
Cost of SECS	3000 $/kW
Rated power of WECS	850 kW
Rated Powers of SECS	10 kW
Conventional unit rated power	500 kW
Cost of Conventional unit	600 $/kW
Cost of storage system`	280 $/kWh

In order to determine the storage requirement of the system, the cyclic behaviour of the system output power has to be taken into consideration.

This is achieved by defining the output states of the output power as P_{av1}, P_{av2} and P_{av3} for the up, medium and down states respectively. The up

state represents when the output power of the renewable resources is greater than average power, the medium state represents the renewable energy output power being equal to or less than the average power, and the down state is when the output power is equal to zero. Application of the proposed classification of the output power of the WECS and SECS yields the results presented in Table 6. Also, the transition rates between the defined power levels are observed and reported in Table 7.

Table 6: average power and the probability.

	State	Power	Probability
1	Up State	415.4618	0.3643
2	Medium state	77.8078	0.3268
3	Down State	0	0.3089

Table7: Transition rate between the power levels.

	1	2	3
1	0.328	0.4867	0.2887
2	0.326	0.2918	0.3567
3	0.346	0.2216	0.3546

In addition to the cost data, the failure and repair rates for each state are shown in Table 8.

Table 8: failure and repair rates.

State	1	2	3
λ_i	0.0136	0.0034	0.0023
μ_i	0.0516	0.03639	0.2149

The state equation of the system is given by

$$
\begin{bmatrix} \dot{p}_1 \\ \dot{p}_2 \\ \dot{p}_3 \\ \dot{q}_1 \\ \dot{q}_2 \\ \dot{q}_1 \end{bmatrix} = \begin{bmatrix} -0.6856 & 0.4867 & 0.2887 & 0.0516 & 0 & 0 \\ 0.326 & -0.7117 & 0.3567 & 0 & 0.03639 & 0 \\ 0.346 & 0.2216 & -0.6477 & 0 & 0 & 0.2149 \\ 0.0136 & 0 & 0 & -0.7236 & 0.4867 & 0.2887 \\ 0 & 0.0034 & 0 & 0.326 & -0.74469 & 0.3567 \\ 0 & 0 & 0.0023 & 0.346 & 0.2216 & -0.8603 \end{bmatrix} \begin{bmatrix} p_1 \\ p_2 \\ p_3 \\ q_1 \\ q_2 \\ q_3 \end{bmatrix}
$$

Lumping states 3, 4, 5 and 5, the resultant state equation is given by

$$
\begin{bmatrix} \dot{p}_1 \\ \dot{p}_2 \\ \dot{q} \end{bmatrix} = \begin{bmatrix} -0.672 & 0.4867 & 0.1084 \\ 0.326 & -0.7083 & 0.1341 \\ 0.3596 & 0.225 & -0.2426 \end{bmatrix} \begin{bmatrix} p_1 \\ p_2 \\ q \end{bmatrix}
\tag{24}
$$

Finally, the solution of the system, assuming that it started in state 3, gives the following equation:

$P_1(t) = 0.0318e^{-1.1157t} - 0.3064e^{-0.4954t} + 0.2746e^{-0.0288t}$

$P_2(t) = -0.0183e^{-1.1157t} - 0.2448e^{-0.4954t} + 0.2631e^{-0.0288t}$

$q(t) = 0.0224e^{-1.1157t} - 0.4060e^{-0.4954t} + 0.5716e^{-0.0288t}$

Using the average output power of each state, the output power at any time is obtained as

$P_o(t) = 11.77e^{-1.1157t} - 146.2504e^{-0.4954t} + 134.48086e^{-0.0288t}$ (25)

The system average return time is obtained at any output level by solving

$$P_L = 11.77e^{-1.1157t} - 146.2504e^{-0.4954t} + 134.48086e^{-0.0288t} \qquad (26)$$

Finally, the average return time and storage capacity Q as a function of the firm levels is shown in Figure 8. This result can be used to estimate the storage capacity required for maintaining different capacity levels. Figure 9 shows the relationship between the total cost of the system and the annual savings at different firm levels. The system benefit-to-cost ratio (BCR) and total savings at different storage capacities are shown in Figure 10. It can be observed that to increase the firm level from 20 kW to 40 kW, the storage capacity has to increase from 500 kWh to 700 kWh. In the same way, the system annual cost has increased from 4.22 $x10^6$ $ to 4.24 $x10^6$ $. It is clear that the overall system savings will increase from 1.91 $x10^6$ $ to 1.97 $x10^6$ $ per annum.

A sensitivity analysis was carried out on the rated power of the wind and solar energy conversion systems. A representative sample of the results is shown in Figure 11. The results show that the BCR of the proposed systems is more sensitive to the rated power of the WECS. Hence increasing the rated power of the WECS increased the BCR of the system more than increasing the rated power of the SECS. Also, the system savings is not sensitive to the rated power of these units. An increase in the

rated power of the renewable energy resources increased the project cost without actually increasing the benefits of the system.

The effects of the capital cost of each unit on the system BCR ratio have been investigated. The study was done with the anticipation that the cost of each unit will decrease in the future(Chowdhury, Chowdhury, & Crossley, 2009). Therefore, it is assumed that the cost decreased by 10, 20 and 30% in each case. In the same way, a sample of the results is shown in Figure 12. The results of the WECS have shown an increase in the BCR of the system by 9.2, 18. 5 and 38.5%. In the case of the SECS, the system BCR increased by 0.07%, 0.14% and 0.2088% in that order. In the same way, the BCR of the system increased by 0.62, 1.34 and 1.76% of the storage system cost. Also, the system BCR increased by 0.42%, 0.85% and 1.27% of the conventional unit cost. It can be seen that in each case, the system BCR increases with decreases in the capital cost. In general, decreases in the capital cost of the WECS system increased the BCR by nearly the same factor. Therefore the best way to increase the benefit of the system is to decrease the capital costs of the WECS.
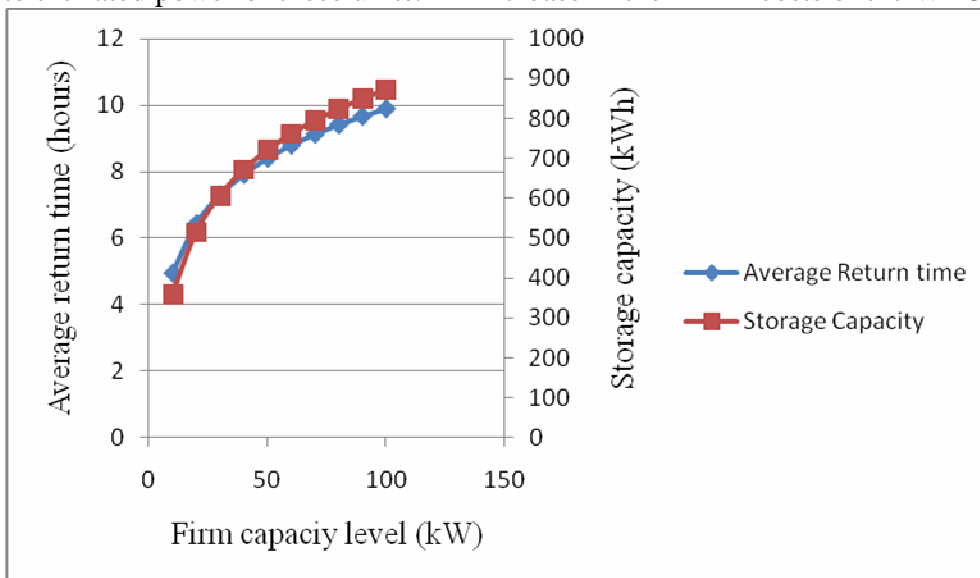

Figure 8: Annual return time and storage capacity at different firm levels.
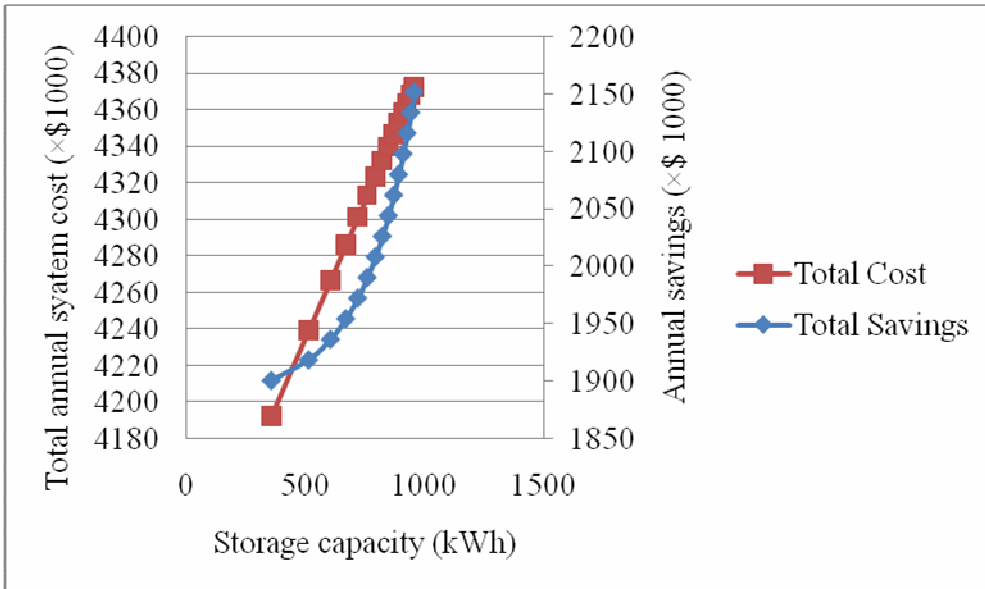
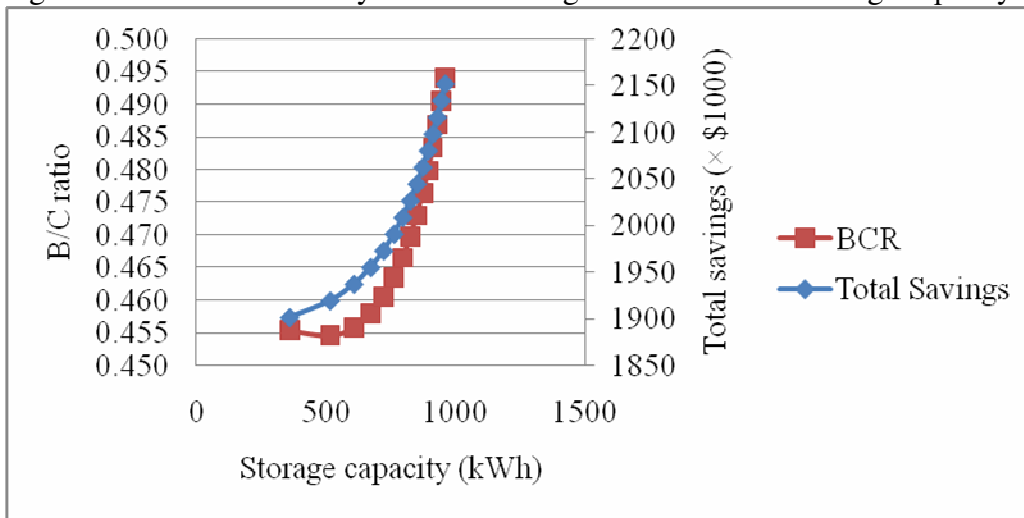Figure 9: Total cost of the system and savings as a function of storage capacity.

Figure 10: BCR and annual savings at different storage capacities.
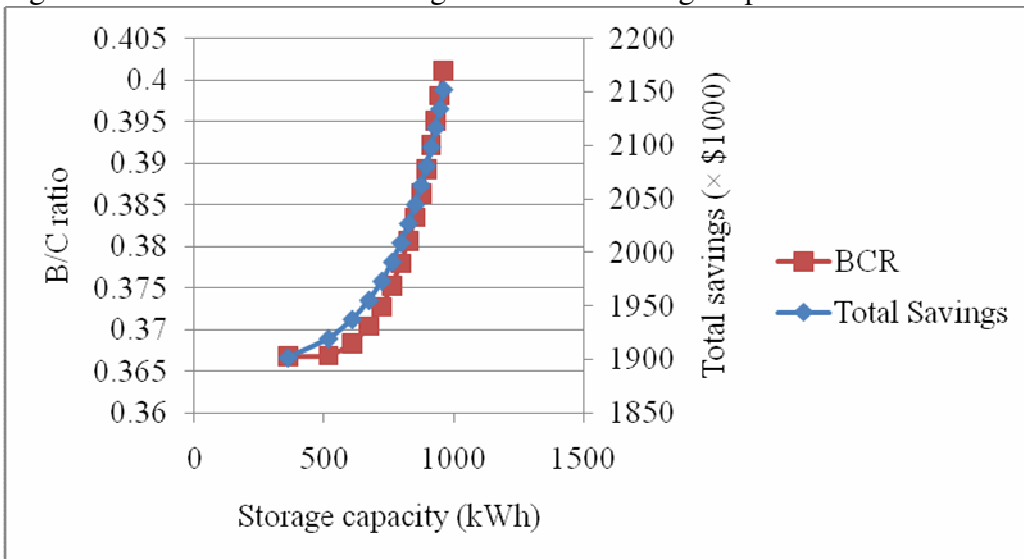

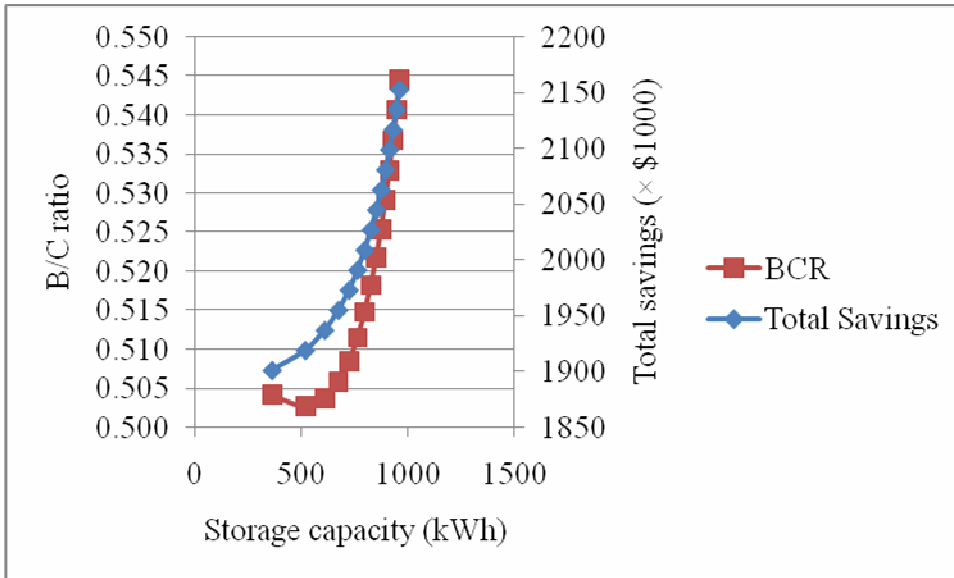Figure 11: Effects of increasing the rated power of WECS by 25%.

Figure 12: Decrease in the capital cost of WECS by 10%.

8. Analysis of system availability using the Boolean logic driven Markov process

A hybrid renewable energy microgrid has many systems that are connected in standby mode. Therefore the availability model of the system is very difficult to obtain. Monte Carlo simulation could have solved the problem. However, it is time-consuming, and the precision of the results has not been determined. Due to the dependence of the proposed microgrid on the weather, conventional methods such as a fault tree may not be suitable. In order to solve these problems, usually papers rely on dynamic models such as Markov processes. In recent applications, higher level methods are now being applied. In order to address all the weaknesses of the existing techniques, a new method that combined the application of the Markov process and of the fault tree called Boolean logic driven Markov process (BDMP) has been proposed. This method has created a compromise among the three available techniques. It has also provided a new graphical representation of the fault tree augmented by a new link represented by a dotted arrow (Carer, Bellvis, Bouissou, & J., 2002), (Bouissoua & Bon, 2003). The procedure is proposed because it uses state transition rates. In addition, it also assumes that the system or equipment failure follows an exponential distribution. Similarly, other parameters, such as switching and repair rates, are within the exponential distribution(Billinton & Bollinger, 2007). One of the benefits of the proposed method is that it is applicable to any size and complexity. The state transition rate or probability is obtained by using the differential equation

$$\frac{dp_i(t)}{dt} = p_i(t)$$

(27)

where $p_i(t)$ = probability of system state i at time t in general. Equation (6.28) can be written in matrix form as

$$\dot{p} = Tp$$

(28)

The solution of the differential equation can be written as

$$p(t) = p_o e^{At}$$

(29)

where p_o is the initial vector of all states.
On the other hand, the exponential of Equation (29) converges absolutely and uniformly to a finite interval of time. In this case, it is assumed that all states with all components in upstate have unity probability while the rest have zero. Therefore, the exponent can be defined as

$$e^{At} = I + AI + A^2 \frac{t^2}{2!} + \cdots = I + \sum_{k=1}^{\infty} A^k \frac{t^k}{k!}$$

(30)

Since our interest is on the final value, the derivative of the equation will be zero. Finally, we have a system of algebraic equations as

$$0 = Tp \tag{31}$$

The determinant of T is zero, meaning that the equations are linearly dependent. Hence one of the equations can be discarded and substituted with Equation (32)

$$\sum_{t=1}^{n} p_t = 1 \tag{32}$$

The system transition matrix can be written as

$$T_n = \begin{bmatrix} t11 & t12 & \cdots & t1n \\ \cdots & \cdots & \cdots & \cdots \\ t(n-1)^1 & t(n-1)^2 & \cdots & t(n-1)^n \\ \cdots & \cdots & \cdots & \cdots \end{bmatrix}$$

and a new steady state equation is obtained as follows:

$$\begin{bmatrix} t11 & t12 & \cdots & t1n \\ \cdots & \cdots & \cdots & \cdots \\ t(n-1)^1 & t(n-1)^2 & \cdots & t(n-1)^n \\ 1 & 1 & 1 & 1 \end{bmatrix} \begin{bmatrix} p_1 \\ \cdots \\ p_{n-1} \\ p_n \end{bmatrix} = b$$

where,

$$b = \begin{bmatrix} 0 \\ \cdots \\ 0 \\ 1 \end{bmatrix}$$

Since the right hand side is no longer zero, it is possible to write the final solution of the steady state equation as Equation (36)

$$p = T_n^{-1} b \tag{36}$$

Finally, Equation (36) gives the probability of every state in the model. Since the microgrid network may be exposed to weather fluctuations, the environment may have considerable effects on system availability. The proposed model is
.

$$T = \begin{bmatrix} t11 & t12 & \cdot\cdot & t1n \\ t21 & t22 & \cdots & t2n \\ \cdots & \cdots & \cdots & \cdots \\ tn1 & tn2 & \cdots & tnn \end{bmatrix} \tag{33}$$

where the off-diagonal elements of T are the failure and repair rates that represent the transitions between the states of the system. The diagonal elements are the transitions out of states with a negative sign. Substituting the nth row of the T matrix, a new equation is obtained as

$$\tag{34}$$

$$\tag{35}$$

assumed to be installed in an environment having normal weather as well as bad weather conditions such as a storm. In order to achieve this, an exponential distribution is assumed. Once the basic assumptions are well understood and the modelling approach is known, it is possible to apply the procedure on a single unit with a two state failure. Figure 13 shows the state space diagram of the single unit with a state fluctuating environment
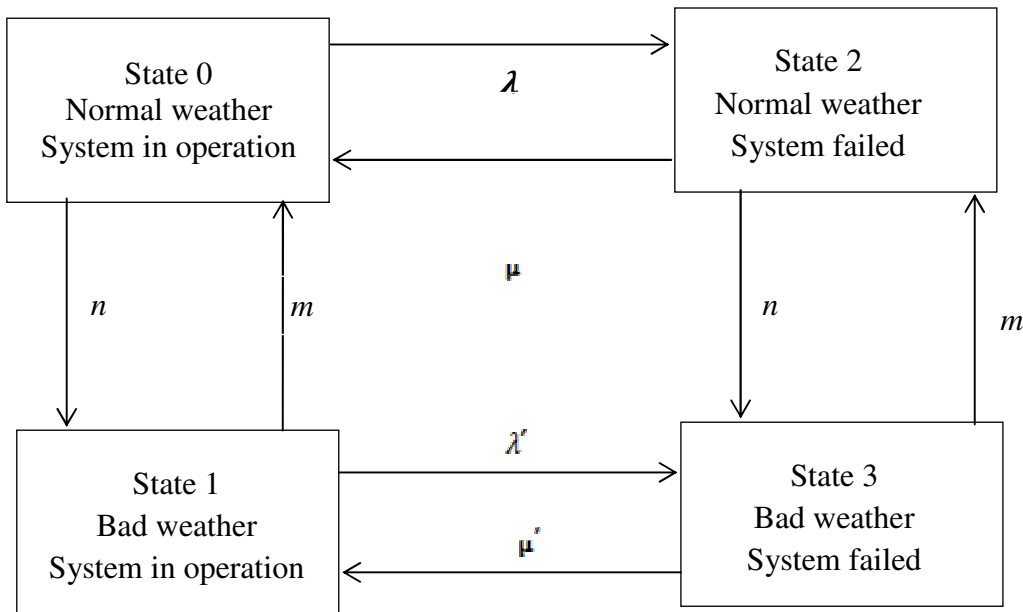
Figure 13: State space diagram of the single unit.

The differential equation of the model is defined as

$$
\begin{bmatrix} p_0(t)' \\ p_1(t)' \\ p_2(t)' \\ p_3(t)' \end{bmatrix} = \begin{bmatrix} -(\lambda+n) & n & \lambda & p' \\ m & -(\lambda'+m) & 0 & \lambda' \\ \mu & 0 & -(n+\mu) & n \\ 0 & \mu' & m & -(\mu'+n) \end{bmatrix} \begin{bmatrix} p_0(t) \\ p_1(t) \\ p_2(t) \\ p_3(t) \end{bmatrix} \qquad (37)
$$

The steady state probabilities of the model are given by

$-(n+\lambda)P_o + mP_1 + \mu P_2 = 0$

$nP_o - (m+\lambda)P_1 + \mu'P_3 = 0$

$nP_o - (\mu+n)P_2 + mP_3 = 0$

$\lambda'P_1 + nP_2 - (m+\mu'[\Box)P]_3 = 0$

and

$P_o + P_1 + P_2 + P_3 = 1$

$P_o + P_1 + P_2 + P_3 = 1$,

P (system availability) = $P_o + P_1$

P (system unavailability)#

$= P_2 + P_3$

The proposed procedure is applied to a hybrid microgrid, and the solution is presented. Initially, it is assumed that the system consists of a diesel generator. This is because isolated loads and communities relied on diesel generators. In this case, the availability of the system is the availability of the diesel generator. The proposed methodology takes into consideration that the system is integrated with wind and solar. Therefore, the model can be presented in the form of the state space model shown in Figure 14.
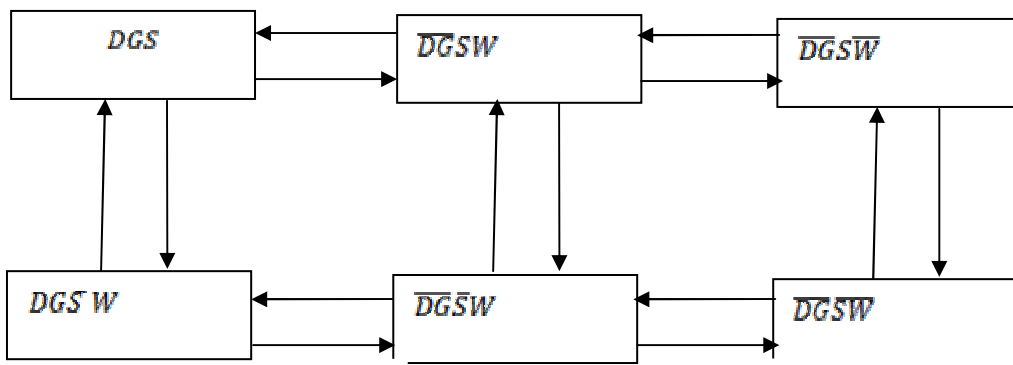
Figure14: State space of microgrid without storage

Application of the procedure above to a microgrid yields the differential equation in matrix form presented in Equation (38)

$$
\begin{bmatrix} p_0(t)' \\ p_1(t)' \\ p_2(t)' \\ p_3(t)' \\ p_4(t)' \\ p_5(t)' \end{bmatrix} = \begin{bmatrix} -(\lambda_s+\lambda_{DG}) & \mu_{DG} & \mu_S & 0 & 0 & 0 \\ \lambda_{DG} & -(\mu_{DG}+\lambda_s+\lambda_w) & 0 & \mu_S & \lambda_w & 0 \\ \lambda_s & 0 & -(\mu_S+\mu_{DG}) & \mu_{DG} & 0 & 0 \\ 0 & \lambda_s & \mu_{DG} & -(\mu_{DG}+\mu_S+\lambda_w) & 0 & \mu_w \\ 0 & \lambda_w & 0 & 0 & -(\lambda_s+\lambda_w) & \mu_S \\ 0 & 0 & 0 & \lambda_w & \lambda_s & -(\mu_S+\mu_w) \end{bmatrix} \begin{bmatrix} p_0(t) \\ p_1(t) \\ p_2(t) \\ p_3(t) \\ p_4(t) \\ p_5(t) \end{bmatrix}
$$

(38)

The failure and repair rates assumed are given in the Table 9. Finally, the differential equation is solved and the result is presented in Equation (39).

Table 9: Annual failure and repair rates of each unit.

Failure rate	Normal weather	Stormy weather	Repair rate
Bat	0.1	0.13	0.25
RE	0.13	0.17	0.27
DG	0.1	0.13	0.4
TR	0.34	0.44	0.02

$$
\begin{bmatrix} p_o \\ p_1 \\ p_2 \\ p_3 \\ p_4 \\ p_5 \end{bmatrix} = \begin{bmatrix} 0.91611 \\ 0.0226 \\ 0.04554 \\ 0.00087 \\ 0.01421 \\ 0.00067 \end{bmatrix}
$$

(39)

It can be seen that the availability of the power supply to the consumer connected to the microgrid is 0.9993308. The unavailability of the network is 0.000669.

9. Effects of weather on the availability
of a standalone microgrid

This section investigates the availability of the microgrid while considering weather conditions. The BDMP model presented in section 9 is modified to accommodate weather factors. Figure 15 shows the new model that considers good and bad weather fluctuations. The differential equation of the network can be defined in Equation (40).

$$P(t) = [p(t)]\begin{bmatrix} D_1 & n[I] \\ m[I] & D_2 \end{bmatrix} \quad (40)$$

where, m and n are the durations of normal and stormy weather, D_1 is a matrix describing the transitions between the normal weather conditions descried in Equation (41), and D_2 is a matrix describing the transitions between the stormy weather conditions defined in Equation (42).

$$D_1 = \begin{bmatrix} -(\lambda_s+\lambda_{DG}+n) & \mu_{DG} & \mu_s & 0 & 0 & 0 \\ \lambda_{DG} & -(\mu_{DG}+\lambda_s+\lambda_w+n) & 0 & \mu_s & \lambda_w & 0 \\ \lambda_s & 0 & -(\mu_s+\mu_{DG}+n) & \mu_{DG} & 0 & 0 \\ 0 & \lambda_s & \mu_{DG} & -(\mu_{DG}+\mu_s+\lambda_w+n) & 0 & \mu_w \\ 0 & \lambda_w & 0 & 0 & -(\lambda_s+\lambda_w+n) & \mu_s \\ 0 & 0 & 0 & \lambda_w & \lambda_s & -(\mu_s+\mu_w+n) \end{bmatrix}$$

(41)

$$D_2 = \begin{bmatrix} -(\lambda'_s+\lambda'_{DG}+m) & \mu'_{DG} & \mu'_s & 0 & 0 & 0 \\ \lambda'_{DG} & -(\mu'_{DG}+\lambda'_s+\lambda'_w+m) & 0 & \mu'_s & \lambda'_w & 0 \\ \lambda'_s & 0 & -(\mu'_s+\mu'_{DG}+m) & \mu'_{DG} & 0 & 0 \\ 0 & \lambda'_s & \mu'_{DG} & -(\mu'_{DG}+\mu'_s+\lambda'_w+m) & 0 & \mu'_w \\ 0 & \lambda'_w & 0 & 0 & -(\lambda'_s+\lambda'_w+m) & \mu'_s \\ 0 & 0 & 0 & \lambda'_w & \lambda'_s & -(\mu'_s+\mu'_w+m) \end{bmatrix}$$

(42)

where λ■ EMBED Equation.DSMT4 ■■■ and μ■ EMBED Equation.DSMT4 ■■■ are the failure and repair rates during a stormy weather condition.
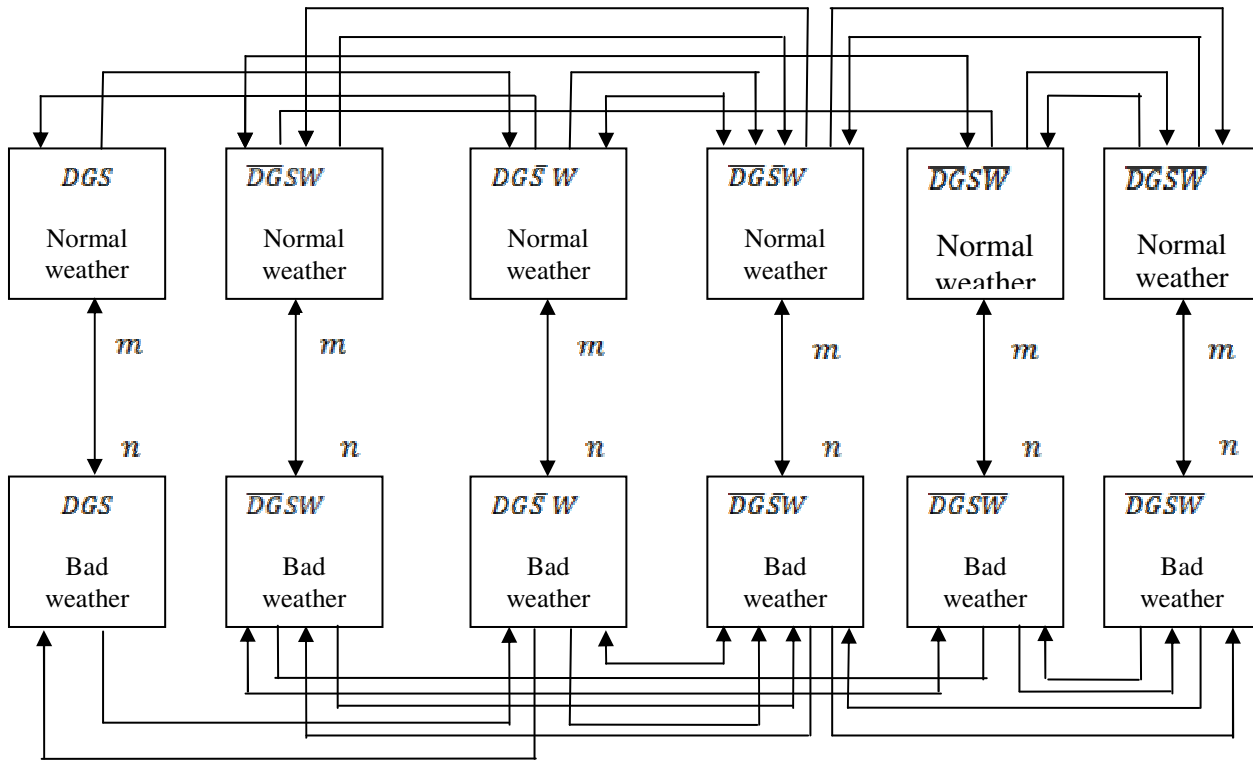
Figure 16: BDMP of the standalaone microgrid.

$$
\begin{bmatrix}
p_O \\
p_1 \\
p_2 \\
p_3 \\
p_4 \\
p_5 \\
P_O{}' \\
P_1{}' \\
P_2{}' \\
P_3{}' \\
P_4{}' \\
P_5{}'
\end{bmatrix}
=
\begin{bmatrix}
0.9161 \\
0.0226 \\
0.0455 \\
0.0009 \\
0.0142 \\
0.0007 \\
0.4654 \\
0.1005 \\
0.2321 \\
0.0409 \\
0.1263 \\
0.0348
\end{bmatrix}
\tag{43}
$$

Hence the availability of the network is obtained by solving the steady state equation. Figure 17 compared the availability of the two models. It can

.

be observed that neglecting weather and its duration could lead to overestimation of the system availability
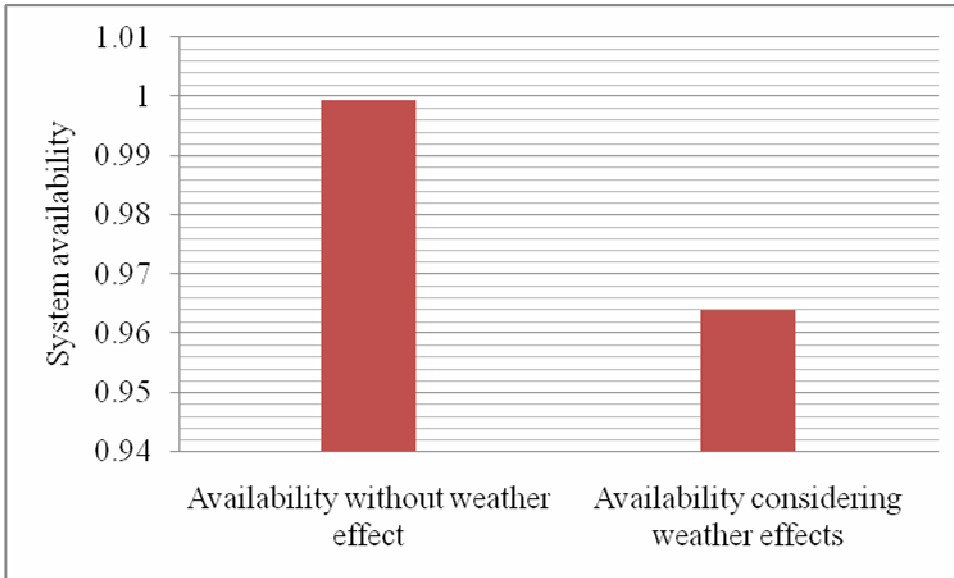
Figure 17: Effects of weather on the availability of a hybrid microgrid.

Another factor that affects the availability of the system is the duration of the normal and bad weather, as shown in Equation (40). The effects of periods of 200, 300, 500 and 1000 hours were studied. The system availability variation with the duration of bad weather is shown in Figure 18. It is observed that the system is very sensitive to the duration of the disturbed weather. The results show that increases in bad weather durations decrease the availability of the system by 5.36%, 9.73% and 13.05%, respectively. Hence system availability is sensitive to the duration of bad weather.
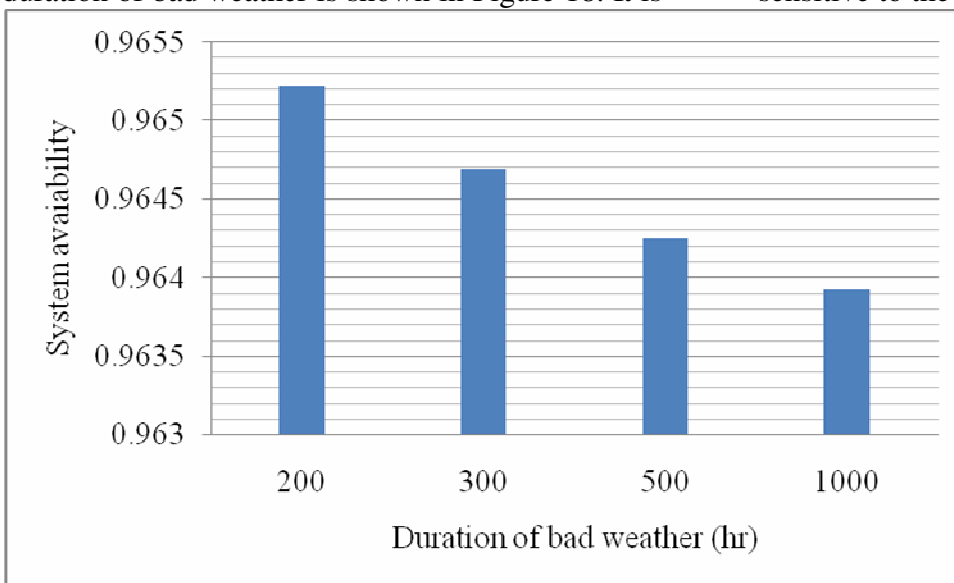

Figure 18: variation of the system availability with bad weather.

10. Conclusion

The output power of the hybrid renewable energy microgrid has been analysed based on the Markov theory. It has been shown that it is possible to preserve the information of the output power of a hybrid renewable energy microgrid statistically. The possibility of using the Markov approach and BDMP in the analysis of a hybrid microgrid has been demonstrated. The results show that increasing the rated power of a SECS is the best way to maximise the benefits of a diesel generator connected to a standalone microgrid. Also, the number of times a diesel generator starts in this proposed system is proportional to the cut-in speed of the wind turbine generator.

An analysis of the storage connected to the system has been carried out by introducing a model that takes the failure and repair rates into consideration. The result shows that it is possible to determine the average return time at the specified output level of the system. This is used to

determine the storage capacity at a specified firm level that causes the WECS and SECS to have a capacity credit. The analysis has shown that increases in the firm level from 100% to 200% require 40% additional capacity for the storage system. This will translate into a 0.5% and 3.14% increase in the capital cost and savings respectively.

Sensitivity analysis of the size factors has shown that the system is more sensitive to the rated power of the WECS. In the same way, the best way to increase the benefits of the system is to decrease the capital costs of the WECS. Also, neglecting weather conditions overestimates system availability by 3.55%. System availability is sensitive to bad weather's duration.

References

bdelkader, S. (2013). Analysis of wind energy conversion system based on Markov state model. *Renewable Power Generation Conference (RPG 2013), 2nd IET*. Beijing.

illinton, R., & Allan, R. (1983). *Reliability evaluation of engineering systems concepts and techniques*. Toronto: Pitman.

illinton, R., & Bollinger, K. (2007). Transmission system reliability evaluation using Markov processes. *IEEE Transactions on power apparatus and systems, PAS-87*(2), 538-547.

ouissoua, M., & Bon, J. (2003). A new formalism that combines advantages of fault-trees and Markov models: Boolean logic driven Markov processes. *Reliability Engineering & System Safety, 82*(2), 1469-163.

arer, P., Bellvis, J., Bouissou, M., & J., D. (2002). A new method for reliability assessment of electrical power supplies with standby redundancies. *Proceedings of the 7th International Conference on Probabilistic Methods Applied to Power Systems (PMAPS'02)*. Suva.

howdhury, S., Chowdhury, S., & Crossley, P. (2009). *S. Chowdhury, S.Microgrid and active distribution networks*. London, United Kingdom: IET.

anco, T., & Testa, A. (2007). A Markovian approach to model power availability of a wind turbine. *Power Tech, IEEE*. Lausanne.

afreshi, S., Zamani, H., Ezzati, S., & Vahedi, H. (2010). Optimal Unit Sizing of Distributed Energy Resources in MicroGrid Using Genetic Algorithm. *Electrical Engineering (ICEE), 18th Iranian Conference on*. Isfahan, Iran.

ang, Y., Pei, W., & Qi, Z. (2012). Optimal sizing of renewable energy and CHP hybrid energy microgrid system. *Innovative Smart Grid Technologies - Asia (ISGT Asia), IEEE*. Tianjin.

hang, L., Barakat, G., & Yassine, A. (2012). Deterministic optimization and cost analysis of hybrid PV/wind/battery/diesel power system. *International journal of Renewable Energy Research, 2*(4), 687-696.

hang, L., Barakat, G., & Yassine, A. (2012). Deterministic Optimization and Cost Analysis of Hybrid PV/Wind/Battery/Diesel Power System. *International journal of Renewable Energy Research, 2*(4), 687-696.

hao, B., Xuesong, Z., Jian, C., Caisheng, W., & Li, G. (2013). Operation Optimization of Standalone Microgrids Considering Lifetime Characteristics of Battery Energy Storage System. *IEEE Transaction on Sustainable Energy, 4*(4), 934-942.

hao, B., Zhang, X., Chen, J., Wang, C., & Guo, L. (2013). Operation Optimization of Standalone Microgrids Considering Lifetime Characteristics of Battery Energy Storage System. *, IEEE Transactions on Sustainable Energy, 4*(4), 934- 943.